Journal of Statistical Physics, Vol. 61, Nos. 1/2, 1990

Superdegenerate Point in FCC Phase Diagram: CVM and Monte Carlo Investigations

R. Tétot,[1,2] A. Finel[1] and F. Ducastelle[1]

Received February 21, 1990; Final May 17, 1990

We investigate the topology of the phase diagram of binary alloys on the fcc lattice with first-neighbor antiferromagnetic interactions around the superdegenerate point, where the $L1_0$ and $L1_2$ phases meet. We treat the system as a "hard-constraint lattice gas," following a procedure previously described by Lebowitz *et al.* We perform cluster variation method calculations in the $T \to 0$ limit and Monte Carlo simulations directly at $T = 0$ K on the ground states of the superdegenerate point. We find that: (i) there is no disordered phase in the neighborhood of this point; (ii) a phase L′ for which two of the four cubic sublattices have the same average occupancy and each of the two others are different appears between $L1_0$ and $L1_2$; (iii) the transition L′/$L1_2$ is of first order.

KEY WORDS: Ising model; superdegenerate ground states; cluster variation method; Monte Carlo simulations; constrained lattice gas.

1. INTRODUCTION

The phase diagram of binary alloys on the fcc lattice with first-neighbor antiferromagnetic interactions J has been greatly studied in the last decade (see refs. 1–11 and references therein). Most of these studies have been mainly concerned with the particular problem of the location of the triple point where the ordered $L1_0$ and $L1_2$ phases and the disordered one meet. The first Monte Carlo simulations by Binder *et al.*[1–3] located the triple point at 0 K, in disagreement with the preceding CVM results of de Fontaine and Kikuchi[4] and the later results of Sanchez *et al.*[5] Nevertheless, the value of the transition temperature given by these CVM

[1] ONERA, BP 72, 92322 Chatillon Cedex, France.
[2] Permanent address: Laboratoire des Composés Non Stoechiométriques, Université Paris Sud, Centre d'Orsay, 91405 Orsay Cedex, France.

0022-4715/90/1000-0121$06.00/0

studies depends on the degree of the approximation used. For this reason, this question remained unsettled for a few years. Since the more recent work by Lebowitz *et al.*,[6] Gahn,[7,8] Ackermann *et al.*,[9] and Diep *et al.*[10] using Monte Carlo simulations, and those by Finel and Ducastelle[11] using CVM, the problem seems to have been solved: the triple point is

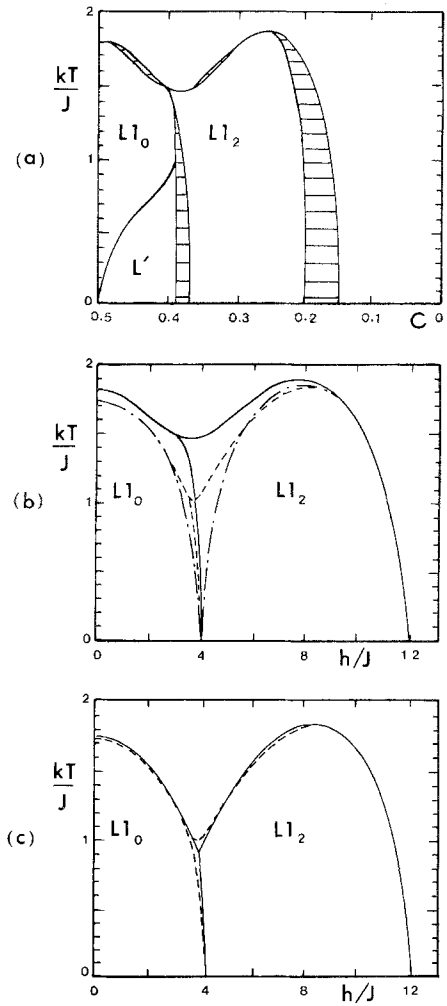

Fig. 1. Phase diagram of the antiferromagnetic fcc lattice. (a) C–T plane: CVM octahedron–tetrahedron (from ref. 11). (b) h–T plane: (—) CVM octahedron–tetrahedron (from ref. 11): for clarity, low temperature features around $h_0 = 4J$ have been omitted (see Fig. 6b); (– – –) Monte Carlo (from ref. 1); (– – –) Monte Carlo (from ref. 10). (c) h–T plane: (—) mixed CVM (from ref. 13); (– – –) Monte Carlo (from ref. 10).

located at finite temperature (even if there is a quantitative difference about its precise location: $T_t = 1.5J$ in CVM and $T_t = J$ in Monte Carlo). For a complete historical review of the controversy on this point, see ref. 12. These results are summarized on the phase diagram reported in Fig. 1. Finally, a CVM phase diagram has been derived, with a new refined approximation.[13] The resulting phase diagram is extremely close to the one obtained by Monte Carlo simulations (see Fig. 1c).

The aim of this paper is not to add one more study on this problem, but to investigate the topology of the phase diagram around the so-called "superdegenerate point" at $T=0$ and $h=4J$, where the ordered $L1_0$ and $L1_2$ phases meet. It can be noted that another superdegenerate point is located at $h=12J$, but is less interesting and will not be discussed here. As pointed out by Lebowitz *et al.*,[6] neither the classical Monte Carlo method nor low-temperature expansions can unambiguously describe the phase diagram around a superdegenerate point. These authors have also shown that, in the limit $T \to 0$, the problem can be translated in terms of a "constrained lattice gas." Following this idea, we have performed CVM calculations in the $T \to 0$ limit and Monte Carlo simulations directly on the ground states at $h=4J$. Three conclusions may be derived from our calculations:

(i) There is no disordered phase in the neighborhood of the superdegenerate point; this confirms that the triple point is located at finite temperature.

(ii) The stability of the phase named L′, first observed in mean-field calculations by Shockley[14] and also present in the CVM results of Finel and Ducastelle[11] (see Fig. 1) is confirmed.

(iii) The transition L′/$L1_2$ is of first order.

2. GENERAL TOPICS

We start with the Ising Hamiltonian

$$H = J \sum_{n,m} \sigma_n \sigma_m - h \sum_n \sigma_n \tag{1}$$

where the first sum runs over the first-neighbor pairs and $\sigma_n = \pm 1$ stands for the usual spin variable. This Hamiltonian also describes binary alloys $A_c B_{1-c}$ with repulsive interactions between atoms of the same species ($J>0$), in which case ordered structures of CuAu ($L1_0$) or Cu_3Au ($L1_2$) type are expected (see Fig. 2). The magnetic field h is then equivalent to the difference between chemical potentials of species A and B and the resulting magnetization $\langle \sigma_n \rangle$ to the difference between the local concentrations.

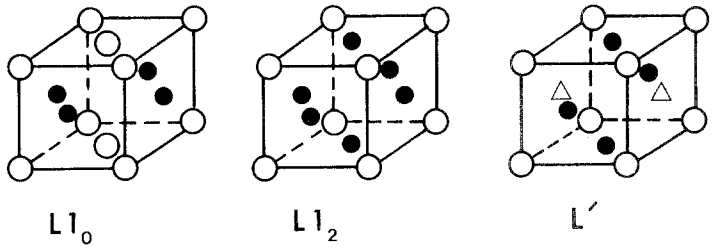

Fig. 2. Ordered structures involved in the phase diagram of Fig. 1.

2.1. Ground States

The ground states of this model have been previously investigated (see refs. 15 and 16 and references therein). They are most easily described in terms of tetrahedron configurations. In short, and except at $h = 4J$ and $h = 12J$, the ground-state energy is obtained with spin configurations which use only one type of first-neighbor tetrahedron (see Fig. 3).

More precisely, for $0 \leqslant h < 4J$ (by symmetry, it is sufficient to consider $h \geqslant 0$), the permitted tetrahedra are those of type AABB (two up spins and two down spins). There is an infinite number of configurations on the fcc lattice which satisfy this criterion: any configuration which consists of (100) planes, antiferromagnetically ordered within the plane but with no order between the planes, is authorized (the well-known $L1_0$ phase belongs to this category). The degeneracy of such a ground state is of order 2^L, where L is the number of (100) planes along one direction. Hence, the residual entropy per site vanishes.

Similarly, for $4J < h < 12J$, the permitted tetrahedra are those of type AAAB, and again this ground state is infinitely degenerate: any configuration with (100) planes alternatively ferromagnetic and antiferromagnetic, with no order between the antiferromagnetic planes, is permitted (the well-

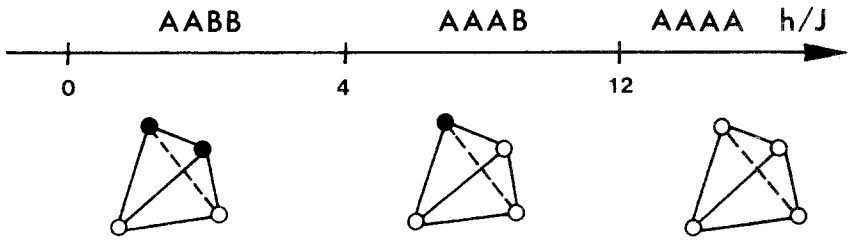

Fig. 3. First-neighbor tetrahedron involved in each h/J region of the phase diagram.

known $L1_2$ phase belongs to this category). As above, the one-dimensional character of this degeneracy leads to a vanishing entropy.

The ground states at the superdegenerate points $h = 4J$ and $h = 12J$ are much more complex. At $h = 4J$, the permitted tetrahedra are simultaneously those of type AABB and AAAB. The degeneracy of this ground state is so high that the residual entropy per site is finite. A lower bound of this entropy may easily be found as follows. The fcc lattice can be divided into four simple cubic sublattices; let two of these sublattices be occupied by A atoms, and one by B atoms. Any configuration obtained by randomly occupying the fourth sublattice is permitted. If N is the number of sites of the fcc lattice, there are $2^{N/4}$ configurations of this type and therefore the residual entropy per site is larger than $\frac{1}{4}\log 2$.

2.2. Low-Temperature Phase Diagram

The low-temperature phases of a system usually correspond to small perturbations of its ground states. This statement is made rigourous within the Pirogov and Sinai theory,[17] together with Slawny's method,[18] under two restrictions: the number of ground states must be finite and a certain criterion of stability must be satisfied (Peierls condition). If these two conditions are satisfied, the phase diagram at sufficiently low temperature is a small perturbation of the zero-temperature one and free energies, and consequently, limits of phase stability can be exactly calculated using standard low-temperature expansions.

These results have been recently extended to situations for which the ground-state degeneracy is infinite, but with no residual entropy.[20, 21] This is precisely the case here for $h < 4J$ and $4J < h < 12J$. The equilibrium states at low temperature correspond to small perturbations of the $L1_0$ phase for $h < 4J$ and of the $L1_2$ phase for $4J < h < 12J$.

The features of the phase diagram around the superdegenerate point $h = 4J$ are much more subtle: as the residual entropy is finite, standard low-temperature expansions cannot be used (in fact, the first problem to solve is precisely the exact determination of this residual entropy). However, it is possible to map this point onto a certain "hard-constraint lattice gas model."[6] This mapping should permit a complete and detailed study of the phase diagram around the superdegenerate point. Our purpose is precisely to investigate numerically this mapping through two different methods, namely CVM calculations and Monte Carlo simulations.

2.3. Hard-Constraint Lattice Gas

According to the procedure described by Lebowitz *et al.*,[6] the Hamiltonian (1) may be rewritten as

$$H = J \sum_{n,m} \sigma_n \sigma_m - h_0 \sum_n \sigma_n - \delta h \sum_n \sigma_n = H_0 - \delta h \sum_n \sigma_n$$

where $h_0 = 4J$, $\delta h = h - h_0$, and H_0 is the Hamiltonian for $h = h_0$.

The partition function is then

$$Z = \sum e^{-H_0/kT} z^{-\sum_n \sigma_n/2} \tag{2}$$

where $z = \exp(-2\delta h/kT)$.

If the temperature is low enough, the first sum runs only over the ground states of H_0, and Z may be rewritten

$$Z(h_0, z) = \sum{}' z^{-\sum_n \sigma_n/2}$$

where the zero of energy is adjusted so that $H_0 = 0$ for a ground state. The prime recalls that the sum is restricted to the ground states of H_0. This partition function can be related to another statistical problem which can be more conveniently described in the lattice gas language with the following variable change:

$$P_n = (1 - \sigma_n)/2$$

Hence, $\sigma_n = -1$ and $\sigma_n = +1$ correspond, respectively, to an occupied site ($P_n = 1$) and an empty site ($P_n = 0$). Then Z becomes

$$Z(h_0, z) = \sum{}' z^{-\sum_n (1 - 2P_n)/2}$$

The upper sum runs over the N sites of the system. Thus

$$Z(h_0, z) = z^{-N/2} \sum{}' z^{\sum_n P_n}$$

$\sum_n P_n$ is the total number of occupied sites n in a particular configuration. So

$$Z(h_0, z) = z^{-N/2} \sum{}' z^n$$

The problem of the limit $T \to 0$, $h \to h_0$ of the initial partition function (2) is equivalent to a lattice gas problem if the quantity $\Theta = \delta h/kT$ is kept constant. The approach to this limit is done along a ray ending at h_0 with a slope Θ (see Fig. 4). In other words, the study of the phase diagram around h_0 can be restricted to the study of a lattice gas with an activity $z = \exp(-2\Theta)$. At $T = 0$, the point $h_0 = 4J$ in the (h, T) plane is related to the segment $\frac{1}{4} \leqslant c \leqslant \frac{1}{2}$ in the (C, T) plane, which corresponds to the variations $[-\infty, +\infty]$ for Θ and $[\infty, 0]$ for z.

This statistical problem falls into the so-called "hard-constraint lattice-gas" type model. Here the constraint is the restriction on the occupation of each tetrahedron. In Sections 3 and 4 we develope the calculations performed using the CVM and Monte Carlo method, respectively. First we present the results provided by the mean-field (Bragg–Williams) theory.

2.4. Mean Field Analysis

As shown elsewhere,[11] a CVM analysis of the phase diagram around the superdegenerate point predicts the stability of a phase, named L′ (see Fig. 2), between $L1_0$ and $L1_2$. In fact, this phase is also present in the classical mean field theory.[14] Within this last approximation, this is due to the fact that this is the only way to get a finite entropy at the superdegenerate point without increasing the ground-state energy. This can be shown as follows.

As mentioned above, the permitted tetrahedra at the superdegenerate point $h_0 = 4J$ have either one or two down spins. In mean field, the probability of observing any configuration on a tetrahedron is given by the product of the site probabilities. More precisely, if $\rho(\sigma_n, \sigma_m, \sigma_p, \sigma_q)$ is the probability that the tetrahedron $nmpq$ has the configuration $(\sigma_n, \sigma_m, \sigma_p, \sigma_q)$, then

$$\rho(\sigma_n, \sigma_m, \sigma_p, \sigma_q) = \rho(\sigma_n) \cdot \rho(\sigma_m) \cdot \rho(\sigma_p) \cdot \rho(\sigma_q)$$

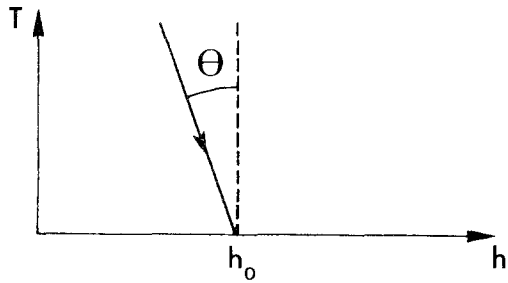

Fig. 4. The approach to the limit $h_0 = 4J$, $T = 0$ is done along a ray of constant slope Θ.

where $\rho(\sigma_i)$ is the probability of observing σ_i at site i:

$$\rho(\sigma_i) = (1 + \sigma_i \langle \sigma_i \rangle)/2$$

where $\langle \sigma_i \rangle$ is the statistical average of the spin variable σ_i.

As a result, if one site of a given tetrahedron is disordered, i.e., $\langle \sigma_i \rangle \neq \pm 1$, the three other sites must be perfectly ordered, with two up spins and one down spin, otherwise some forbidden tetrahedron configurations would have finite probabilities. In other words, in the limit where h and T approach the superdegenerate point, the 12 first neighbors of a disordered site are necessarily ordered, i.e., $\langle \sigma_i \rangle = \pm 1$; moreover, eight of those neighbors must be characterized by $\langle \sigma_i \rangle = +1$ and the four others by $\langle \sigma_i \rangle = -1$. But, up to that point, this observation is only a local rule that describes the first-neighbor configuration of a disordered site. In particular, it does not say if these disordered sites do exist in the equilibrium state and, if so, where they sit in the lattice. For that purpose, we must consider the mean-field free energy at finite T around the superdegenerate point.

In the mean-field approximation, the free energy of our model is

$$F(\{\langle \sigma_i \rangle\}) = J \sum_{n,m}{}' \sigma_n \sigma_m - h \sum_n \langle \sigma_n \rangle - kT \sum_n \left(\frac{1 + \langle \sigma_n \rangle}{2} \log \frac{1 + \langle \sigma_n \rangle}{2} + \frac{1 - \langle \sigma_n \rangle}{2} \log \frac{1 - \langle \sigma_n \rangle}{2} \right)$$

where the first sum runs over first-neighbor pairs. The equilibrium state is obtained when the first derivatives of $F\{\langle \sigma_i \rangle\}$ vanish. As usual, these equations can be written

$$\langle \sigma_n \rangle = \tanh \beta \left(h - J \sum_{m \neq n} \langle \sigma_m \rangle \right) \tag{3}$$

where the sum runs over the 12 first neighbors of site n.

As suggested above, we continue the analysis of these equations, as $h \to h_0 = 4J$ and $T \to 0$, along rays of constant slope Θ (see Fig. 4). The mean-field equations (3) become

$$\langle \sigma_n \rangle = \tanh(\Theta + \beta h_n^{\text{eff}}) \tag{4}$$

with

$$h_n^{\text{eff}} = h_0 - J \sum_{m \neq n} \langle \sigma_m \rangle$$

The term h_n^{eff} plays the role of an effective field which acts on site n. As we approach the superdegenerate point, two situations may occur: $\lim\langle\sigma_n\rangle = \pm 1$ or $\lim\langle\sigma_n\rangle \neq \pm 1$.

1. $\lim_{T\to 0}\langle\sigma_n\rangle = \pm 1$. This is only possible if $\lim \beta h_n^{\text{eff}} = \pm\infty$ [see Eq. (4)]. Hence, we have, as $T \to 0$ along the ray of slope Θ,

$$\langle\sigma_n\rangle \sim \tanh \beta h_n^{\text{eff}} \sim S_n[1 - 2\exp(-2\beta\,|h_n^{\text{eff}}|)] \tag{5}$$

where S_n is equal to the sign of h_n^{eff}.

2. $\lim_{T\to 0}\langle\sigma_n\rangle \neq \pm 1$. If a site n is disordered at zero temperature, its 12 first neighbors m must be perfectly ordered at the superdegenerate point (see discussion above): $\langle\sigma_m\rangle = +1$ for eight of them and $\langle\sigma_m\rangle = -1$ for the four others. More precisely, each of these $\langle\sigma_m\rangle$ must obey, in the limit $T \to 0$, a law given by Eq. (5). As a result, the effective field h_n^{eff} is given by

$$h_n^{\text{eff}} \sim 2J \sum_{m\neq n} S_m \exp(-2\beta\,|h_m^{\text{eff}}|)$$

where the sum runs over the first neighbors of n. The effective fields h_m^{eff} which act on these first neighbors correspond to the first case: $\beta h_m^{\text{eff}} \to \pm\infty$ as $T \to 0$. Hence, $\beta h_n^{\text{eff}} \to 0$ as $T \to 0$. Finally, the mean occupation $\langle\sigma_n\rangle$ of a disordered site approaches the finite value $(\tanh\Theta)$ as

$$\langle\sigma_n\rangle \sim \tanh\Theta + \beta h_n^{\text{eff}}(1 - \tanh^2\Theta) \tag{6}$$

As a result, Eqs. (5)–(6) show that, as we approach the superdegenerate point along a ray of constant slope Θ, the difference between a mean occupation $\langle\sigma_n\rangle$ and its limit value decreases exponentially as $T \to 0$ whether the site n is disordered or not. The same conclusion holds for the difference between the internal energy of any state which contains simultaneously ordered and disordered sites (provided the previous local rules are satisfied) and the ground-state energy at the superdegenerate point. However, and this is the key point, the entropy contribution of a site n depends drastically on whether n is disordered or not. If $\langle\sigma_n\rangle$ behaves as in Eq. (6), its entropy contribution to the free energy, is to the leading order, linear in T:

$$kTs_n \sim -kT\left(\frac{1+\tanh\Theta}{2}\log\frac{1+\tanh\Theta}{2} + \frac{1-\tanh\Theta}{2}\log\frac{1-\tanh\Theta}{2}\right)$$

where $(1+\tanh\Theta)/2 = C_n$ is the concentration of a disordered site, whereas the entropy contribution is exponentially small when $\langle\sigma_n\rangle$ behaves as in Eq. (5):

$$kTs_n \sim 2\,|h_n^{\text{eff}}|\exp(-2\beta\,|h_n^{\text{eff}}|)$$

Thus, for any value of Θ, there is a temperature $T(\Theta)$ below which the entropy gain due to the substitution of an ordered site by a disordered one is larger than the increase of internal energy (if $\Theta \neq 0$, the introduction of a disordered site necessarily increases the internal energy). Hence, the larger the number of disordered sites, the smaller the free energy. However, we cannot introduce more than one disordered site per tetrahedron. Consequently, the minimum energy is reached by any state which contains only tetrahedra of type $++-o$, where the symbol "o" represents a disordered site. Very simple packing arguments show that there is an infinite number of such states, the simplest one being the L′ phase (see Fig. 2). All the disordered sites are then on the same cubic sublattice. The other states can be obtained from L′ by translating any set of parallel (100) planes.

To summarize, the mean-field analysis leads to the following conclusion: as we approach the superdegenerate point $h_0 = 4J$ along a ray of constant slope Θ, the equilibrium state for sufficiently small T corresponds to the L′ phase. This yields the phase diagram of Fig. 5.

We recall that the key point which led us to this result is that, within the mean-field approximation, the 12 first neighbors of a disordered site are necessarily perfectly ordered, and that this fact is a direct consequence of the factorization of the tetrahedron probabilities into site probabilities.

3. CVM CALCULATIONS

It has long been known that the CVM is a very precise technique for studying statistical problems on lattices, provided the basic clusters upon which the algorithm is built are large enough. Basically, a CVM study consists in minimizing a free energy functional where the exact entropy

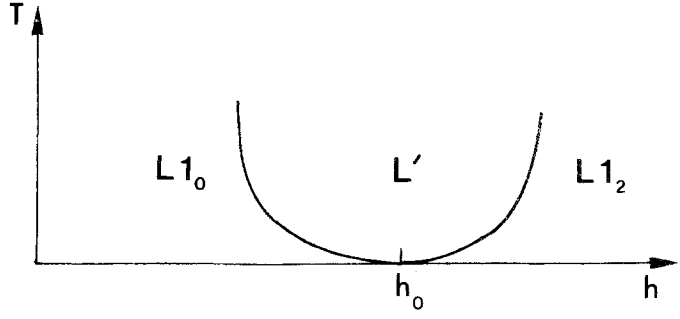

Fig. 5. Phase diagram obtained by the mean-field approximation. When one approaches the limit $h_0 = 4J$, $T = 0$ along a ray of constant slope Θ, there always exists a temperature under which L′ is the most stable phase.

has been replaced by a linear combination of entropies of finite clusters included in a given basic cluster. Consequently, the configurational probabilities of this basic cluster and its subclusters directly enter the CVM free energy functional.

Due to frustration effects with antiferromagnetic first-neighbor interactions, we know that the smallest basic cluster that leads to an overall correct phase diagram is precisely the first-neighbor tetrahedron. Within the tetrahedron (or a larger cluster) approximation, the tetrahedron probabilities are not factorized. Thus, contrary to the mean-field situation, two first-neighbor sites may be simultaneously disordered without increasing the ground-state energy. This is essential for our discussion, as now the stability of the L′ phase is no longer the only way of getting the residual entropy at the superdegenerate point. In particular, the L′ phase could disappear for the benefit of partially disordered $L1_0$ and $L1_2$.

We first present the CVM results in the tetrahedron approximation. As above, we approach the superdegenerate point along rays of constant slope Θ. A special code has been derived to minimize the CVM free energy in the limit $T \to 0$. Our results concerning the phase diagram are summarized in Fig. 1 and 6b. The first point is that the L′ phase has disappeared on the right of the superdegenerate point. More precisely, for $\Theta > \Theta_c$, with $\Theta_c \sim -0.33$, the equilibrium state corresponds to the partially disordered $L1_2$ phase. On the other hand, L′ does exist on the left of the superdegenerate point. Indeed, for $\Theta < \Theta_c$, L′ is more stable than the partially disordered $L1_0$ phase. In short, as Θ increases from $-\infty$ to $+\infty$, the equilibrium state in the limit $T \to 0$ corresponds first to the L′ phase and, through a first-order transition at $\Theta = \Theta_c$, switches to the partially disordered $L1_2$ phase. Concerning the transition $L'/L1_0$, which must exist according to the low-temperature expansion that predicts the stability of $L1_0$ for $h < h_0$ at sufficient small T (see above), we have found a second-order transition.

Finally, we present in Fig. 6a our CVM results concerning the residual entropy $s(\Theta)$, the limit concentration $C(\Theta)$, and the order parameters of L′ and $L1_2$, as functions of $\Theta(T=0)$. We mention first that each site of L′ and $L1_2$ is partially disordered at $T=0$ (in the mean-field analysis, only one of the cubic sublattices was disordered). Note the jump in the residual entropy, which marks the first-order transition at $\Theta = \Theta_c$. We report also in Fig. 6a the residual entropy of the metastable $L1_0$ phase in order to show that the difference from the entropy of the L′ phase is very small. As expected, the residual entropy is maximum for $\Theta = 0$, with $s(\Theta=0) = 0.328 \log 2$. In the tetrahedron-octahedron approximation, we have found $s(\Theta=0) = 0.333 \log 2$.[11] These results are in good agreement with the value $0.345 \log 2$ found in the Monte Carlo simulations of ref. 22.

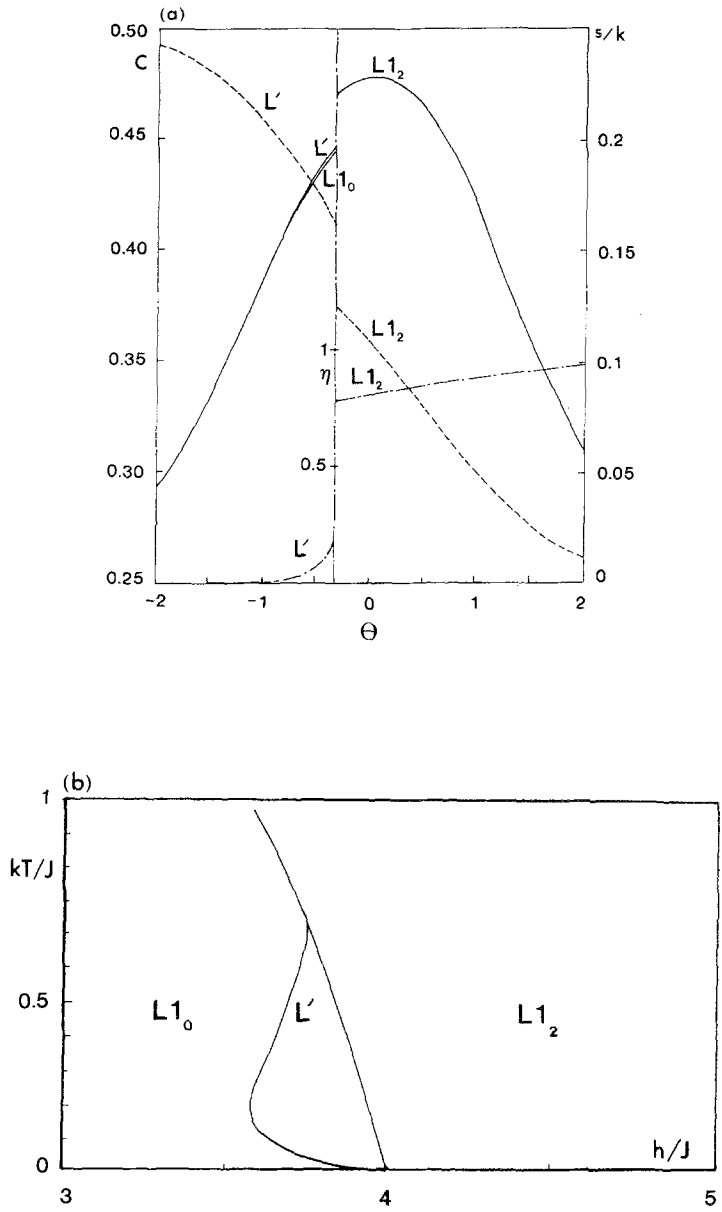

Fig. 6. CVM results around $h_0 = 4J$ as function of Θ. (—), Residual entropies $s(\Theta)$ for $L1_0$, $L1_2$, and L′. (– – –), Limit concentrations $C(\Theta)$ for L′ and $L1_2$. (–·–), Order parameters $\eta(\Theta)$ for L′ and $L1_2$; $\eta_{L'} = C_3 - C_4$, $\eta_{L1_2} = C_1 - C_4$ [C_i, $i = 1$–4, are mean sublattice concentrations $(1 + \langle \sigma_i \rangle)/2$]. (b) CVM phase diagram in the h–T plane.

To summarize, the L′ phase is still present in the CVM analysis. However, its domain of stability is smaller than in the mean field approximation. Thus, we may argue that the stability of this phase could be an artefact of the approximate method used to analyze the equilibrium state around the superdegenerate point, and that L′ would disappear with a higher-order approximation. This does not seem to be the case, as a CVM analysis in the tetrahedron–octahedron approximation leads to a larger domain of stability than in the tetrahedron one.[11] However, even if this observation is a strong indication, it does not prove definitely the stability of L′. In fact, this phase has never been observed in Monte Carlo simulations. But we wish to comment upon two points. First, as the equilibrium states around the superdegenerate point are necessarily partially disordered, it is difficult, with standard Monte Carlo algorithms, to guess the symmetry of the equilibrium state through the observation of particular configurations, but accurate statistical averages on appropriate sublattices (here, the simple cubic ones) may give precise indications. Second, the differences of free energy between L′ and $L1_0$ are extremely small (as an example, for $h = 3.75J$ and $kT = 0.25J$, the CVM free energies per site are $f_{L'} = -2.0131961J$ and $f_{L1_0} = -2.0131945J$). This difference is of the order of $10^{-6}J$. Of course, the CVM is not expected to yield absolute free energies with such a high degree of accuracy; nevertheless, the difference is significant, each free energy being calculated with an accuracy better than $10^{-10}J$.

For these reasons, very long Monte Carlo runs on large samples are necessary both to reach the true equilibrium states and to compute accurate statistical averages. Moreover, we are interested in the limit $T \to 0$, i.e., in a regime where the relaxation process is very slow. In order to overcome these difficulties, a special Monte Carlo code running directly at $T = 0$ has been derived. The procedure and the results obtained are described in the next section.

4. MONTE CARLO SIMULATIONS

In the lattice gas language, as already seen above, each tetrahedron of the fcc lattice should be in only one of the two following states: state 1 when only one site is occupied and state 2 when two sites are occupied. The probability of modifying the occupation of a site is linked to the activity $z = \exp(-2\Theta)$. Two cases have to be distinguished according to the value of z:

(i) When $z < 1$, a vacant site surrounded by eight tetrahedra in state 1 may be filled with probability z and an occupied site surrounded by eight

tetrahedra in state 2 must be emptied (the probability is $1/z > 1$). A site of any other type cannot be modified.

(ii) When $z > 1$, a vacant site surrounded by eight tetrahedra in state 1 must be filled (the probability is $z > 1$) and an occupied site surrounded by eight tetrahedra in state 2 may be emptied with probability $1/z$. A site of any other type cannot be modified.

Therefore, the heart of the program consists in keeping up to date two files containing respectively the sites which must be emptied (or filled) and those which are only available to be filled (or empty). In that way, only

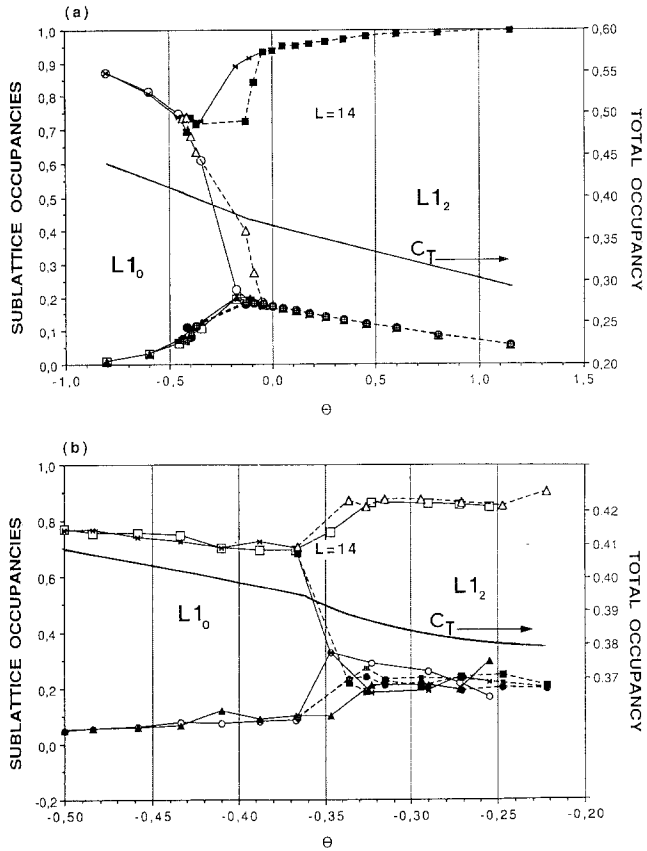

Fig. 7. Monte Carlo average occupancies of the four simple cubic sublattices as functions of Θ for $L = 14$. The calculations have been performed by starting from perfect $L1_0$ (solid lines with □, ○, ▲, ×) and perfect $L1_2$ (dashed lines with ■, △, ●, ⊞). The solid line represents the total average occupancy C_T. (a) The increment of z between two points is 0.1. (b) The increment of z between two points is 0.02.

permitted configurations are visited. Consequently, the relaxation process toward the equilibrium state is much shorter than in classical Monte Carlo simulations. Moreover, the use of helicoidal boundary conditions along x and y axes and periodic ones along the z axis has made it possible to optimize the vectorization of the code. With the classical Metropolis algorithm,[23] the program runs at a rate of about 3×10^6 spin flips per second on a Cray X-MP supercomputer. Simulations have been made with lattice sizes from $L = 14$ to $L = 34$, L being the number of fcc cells along the three axes (the total number of sites is $4L^3$). Generally, for a given z, 5000 Monte Carlo steps per site (MCS) were executed. As less than 1000 MCS are sufficient to reach the equilibrium, the first 1000 MCS were discarded and the next 4000 were used to calculate the average occupancies C_i of the four cubic sublattices. At the end of each run, the last configuration was stored and used as a starting point for the next run with a new value of z.

In Fig. 7a are shown the variations of C_i ($i = 1$–4) and of the total occupancy $C_T = (C_1 + C_2 + C_3 + C_4)/4$ as a function of Θ obtained with $L = 14$. At first sight, a single transition occurs between $L1_0$ and $L1_2$. Figure 7b shows the results obtained more accurately with a smaller increment of z, in the vicinity of the transition. This transition seems to be of first order on account of the sharp variations of the C_i, though no discontinuity appears on C_T. No disordered phase is present, which definitively

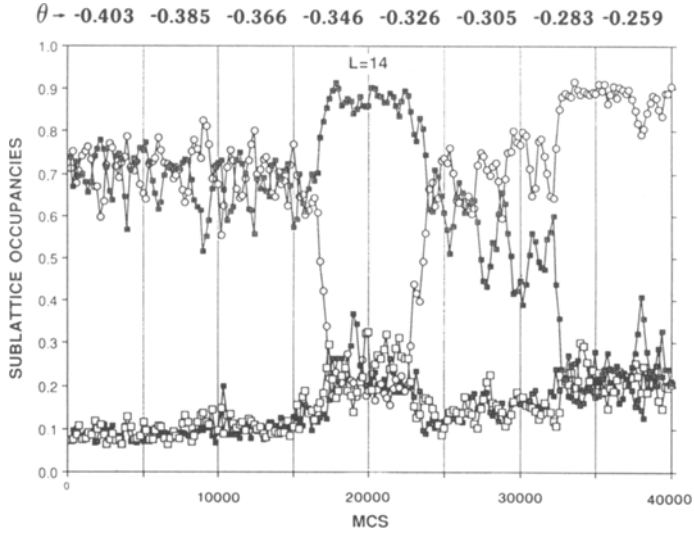

Fig. 8. Temporal variations of the four sublattice occupancies (□, ⊞, ◘, ○) with $L = 14$ for different increasing values of Θ. A point is the average of 200 MCS, 5000 MCS being performed for each value of Θ. Note the sublattice switchings after the transition occurs.

solves the problem of the location of the triple point. A deeper analysis of the transition is prevented by the very large temporal fluctuations and sublattice switchings, as shown in Fig. 8. Hence, larger lattices have been used in order to reduce these effects. In Fig. 9 are presented the temporal fluctuations of C_i ($i = 1$–4) for $L = 20$. Note first the appearance of a hysteresis, which confirms that the transition is effectively of first order. On the other hand, the fluctuations are largely reduced compared to the preceding case, $L = 14$. We observe that the fluctuations are greater for the two sets of sublattices with $C_i \sim 0.7$ and $C_i \sim 0.25$ than for the others ($C_i \sim 0.1$ and $C_i \sim 0.9$) and this is independent of the nature of the phase, $L1_0$ or $L1_2$.

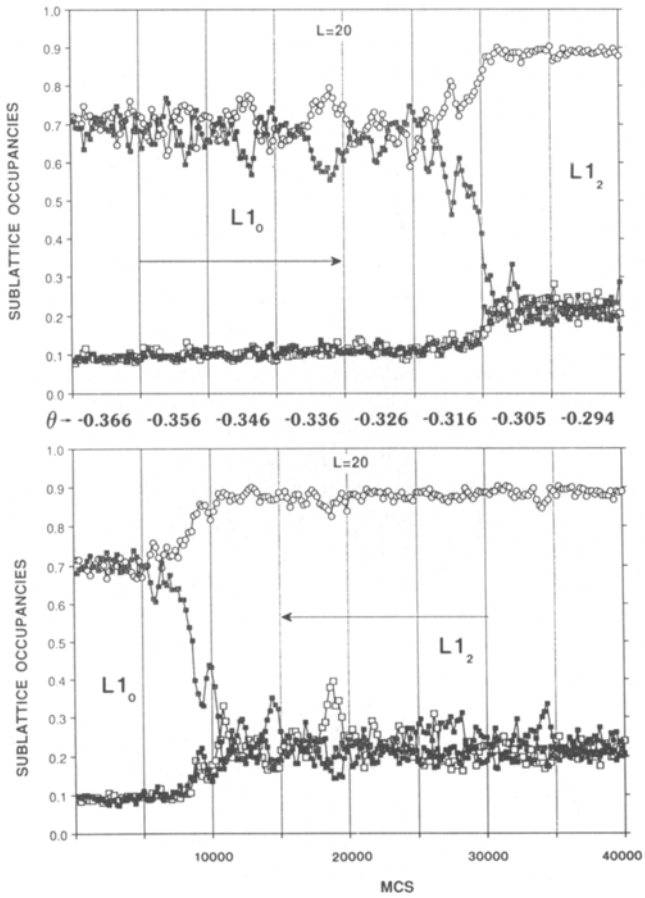

Fig. 9. Same as Fig. 8, for $L = 20$ (arrows show the sense of variation of Θ). Note the hysteresis between the two sets of results corresponding to increasing and decreasing values of Θ.

The fluctuations become weaker when the occupancy approaches the limits 0 and 1. This can be understood with the following simple argument. Intuitively, one feels that the fluctuations on C_i are related to the configurational entropy per site on the sublattice i, which may be expressed as $s_i/k = -[C_i \log C_i + (1-C_i)\log(1-C_i)]$ if a random distribution is assumed. The maximum of this function is obtained for $C_i = 0.5$. Therefore, according to this crude approach, the fluctuations of C_i must increase when $|0.5 - C_i|$ decreases, as observed. Moreover, it can be seen in Fig. 9 that the fluctuations are greater within the boundaries of the hysteresis than outside. In this region, sublattice switchings delimit what we shall call "bubbles" hereafter. Note that these bubbles are larger on the $L1_0$ side than on the $L1_2$ side. The occupancies of the two concentrated sublattices, say C_3 and C_4, are often well separated during a few thousand MCS. According to the mean-field and CVM results presented above, it is inviting to explain these features by the presence of the L′ phase. If this hypothesis is correct, the sublattice switchings would be due to a size effect and should disappear in a sufficiently large lattice. On the other hand, it is also possible that these bubbles correspond to early signs of the transition and do not indicate the stability of any other phase.

In order to study the size effect on this point, we have used lattices with $L = 30$ and $L = 34$. Results corresponding to $L = 30$ are reported in Fig. 10a. This size leads to new results which are not improved by the use of $L = 34$. The situation clearly appears different in the two branches of the hysteresis. On the $L1_0$ branch, bubbles between the two concentrated sublattices C_3 and C_4 are wider and wider and more extended when one approaches the transition and, just before, sublattice switchings vanish and show clearly the L′ phase. Its stability has been checked by performing 15,000 MCS during which neither transition nor sublattice switching was observed. We expect that the two sublattices would be separated sooner with much larger lattices. Nevertheless, computer time needed to do that seems too prohibitive in relation to the importance of the expected results. In particular, when one goes to the transition, the concentration difference $|C_3 - C_4|$ continuously increases to become larger than the statistical error. This can be seen more precisely in Fig. 10b.

In fact, $|C_3 - C_4|$ would represent the order parameter $\eta_{L'}$ of the phase L′ if there were no sublattice switching. This means that L′ exists in a region where the sublattices are not definitively split. $\eta_{L'}$ can be roughly estimated as the average width of bubbles. This is plotted against Θ in Fig. 11. The important point is that $\eta_{L'}$ has a significant nonzero value outside the hysteresis, which proves that L′ is more stable than $L1_0$ in a certain region $\Theta < \Theta_c$. Due to the statistical fluctuations, the limit of this region is difficult to determine within a Monte Carlo procedure.

Nevertheless, the good agreement with the CVM results on this point (see the comparison of $\eta_{L'}$ by the two methods in Fig. 6a and Fig. 11) allows us to suppose that the overall CVM results are qualitatively trustworthy, in particular the prediction of the stability of L′ phase against $L1_0$ in the whole domain $\Theta < \Theta_c$ (see Section 3). In Fig. 11, the plot of C_T versus Θ shows a hysteresis, in complete agreement with the critical value $\Theta_c = -0.333$ given by CVM calculations. The concentration width of the corresponding two-phase region is very small (~ 0.005), which is in

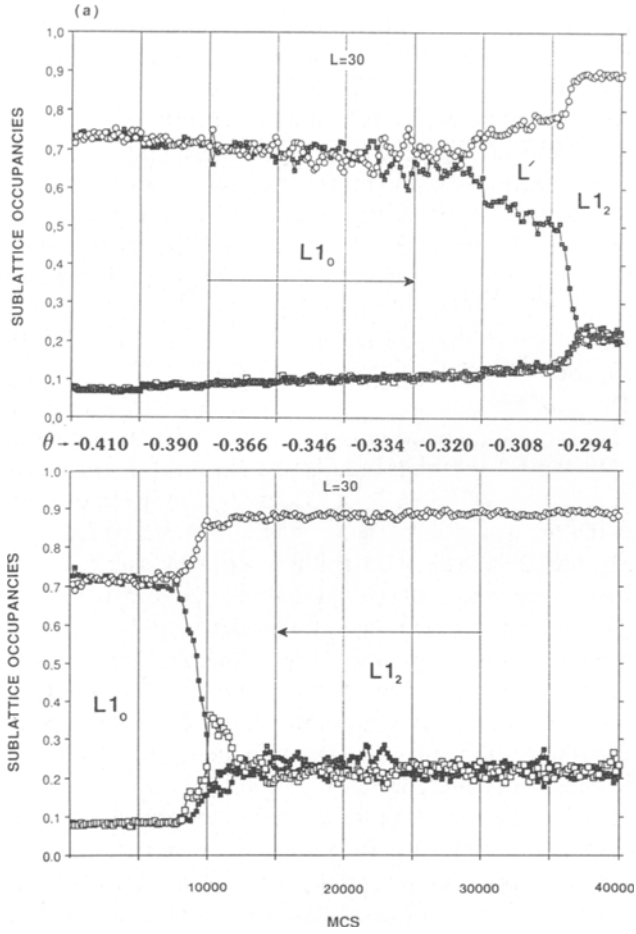

Fig. 10. (a) Same as Fig. 9, for $L = 30$. The remarkable feature is the stable separation between the two concentrated sublattices in the upper part of the figure which shows the stabilization of the L′ phase before the transition. (b) Enlargement of the upper part of part (a), which shows the increase in bubble size when one approaches the transition.

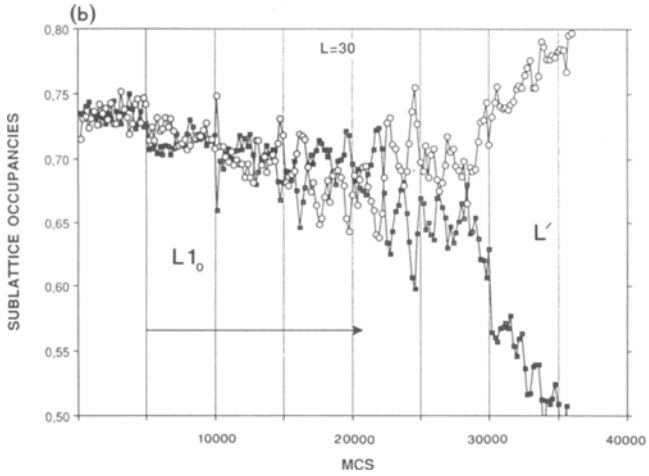

Fig. 10. (*Continued*)

agreement with the Monte Carlo results by Diep *et al.*,[10] although the limit concentrations of this domain ($0.387 \leqslant C_T \leqslant 0.392$) are slightly smaller than theirs. Note that the CVM gives a larger domain ($0.374 \leqslant C_T \leqslant 0.41$). Nevertheless, the limits are different by less than 4% from the Monte Carlo ones. The order parameter of the phase $L1_2$ is also plotted in Fig. 11.

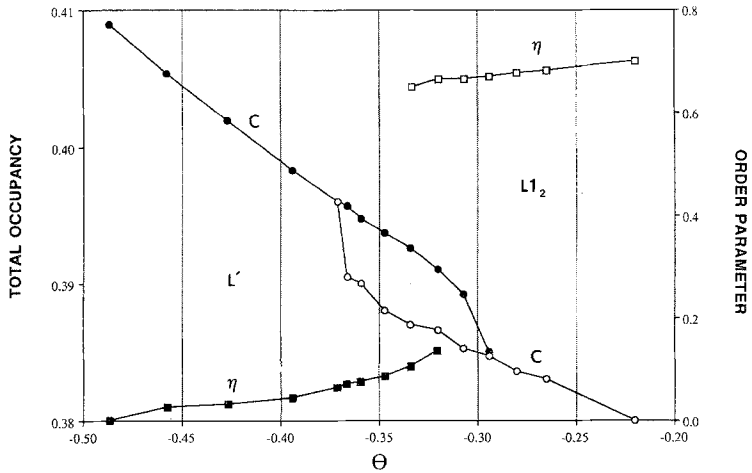

Fig. 11. Monte Carlo results around the superdegenerate point $h_0 = 4J$ as function of Θ. (●) Total occupancy $C_T(\Theta)$ starting from $L1_0$ side, (○) total occupancy $C_T(\Theta)$ starting from $L1_2$ side, (□, ■) order parameter of $L1_2$ and L′.

To summarize, CVM results presented in Section 3 are globally confirmed by the Monte Carlo simulations. The agreement is particularly good for Θ_c and $\eta_{L'}$. The limit concentrations of the two-phase domain differ by less than 4%, and the largest discrepancy concerns the order parameter of the $L1_2$ phase, which is ~ 0.7 in Monte Carlo and ~ 0.82 in CVM.

5. CONCLUSION

The topology of the fcc phase diagram with first-neighbor antiferromagnetic interactions around the superdegenerate point $h = 4J$ has been investigated by means of CVM and Monte Carlo calculations. The two methods lead to the same results. This shows once more the reliability of the CVM technique to study lattice statistics problems with short-range interactions. Our main conclusions are the following. First, there is no disordered phase in the neighborhood of the superdegenerate point; this proves definitively that the triple point is located at finite temperature. Second, there is a first-order transition between L′ and a partially disordered $L1_2$ phase. Concerning this last point, a very precise analysis has shown that the L′ phase is more stable than $L1_0$. This phase has been observed with Monte Carlo simulations for the first time. This observation requires the use of large lattices of more than 100,000 sites and at least 5000 MCS. Nevertheless, it is not possible to determine precisely the domain of existence of this phase by Monte Carlo. On the other hand, owing to its analytical character, the CVM allows one to show that L′ is always more stable than $L1_0$ at 0 K, the difference between the free energies being very small. To be complete, note that a partially disordered phase PD similar to the L′ phase has been observed by Monte Carlo simulations in the triangular Ising model with nearest- and next-nearest-neighbor antiferromagnetic interactions (see ref. 24 and references therein). This phase appears between the 2×1 and 2×2 phases (similar to $L1_0$ and $L1_2$ in this study) near the superdegenerate point $h = 3J_1$.

REFERENCES

1. K. Binder, *Phys. Rev. Lett.* **45**:811 (1980).
2. K. Binder, J. L. Lebowitz, M. K. Phani, and M. H. Kalos, *Phys. Rev. B* **21**:4027 (1980).
3. K. Binder, J. L. Lebowitz, M. K. Phani, and M. H. Kalos, *Acta Met.* **29**:1655 (1981).
4. D. de Fontaine and R. Kikuchi, *Nat. Bur. Std. SP* **496**:999 (1977).
5. J. M. Sanchez, D. de Fontaine, and W. Teitler, *Phys. Rev. B* **26**:1465 (1982).
6. J. L. Lebowitz, M. K. Phani, and D. F. Styer, *J. Stat. Phys.* **38**:413 (1985).
7. U. Gahn, *J. Phys. Chem. Solids* **43**:977 (1982).
8. U. Gahn, *J. Phys. Chem. Solids* **47**:1153 (1986).
9. H. Ackermann, S. Crusius, and G. Inden, *Acta Met.* **34**:2311 (1986).

10. H. T. Diep, A. Ghazali, B. Berge, and P. Lallemand, *Europhys. Lett.* **2**:603 (1986).
11. A. Finel and F. Ducastelle, *Europhys. Lett.* **1**:135 (1986); erratum **1**:543 (1986).
12. R. Kikuchi, *Prog. Theor. Phys. Suppl.* **87**:69 (1986).
13. A. Finel, in *Alloy Phase Stability*, G. M. Stocks and A. Gonis, eds. (Kluwer, Dordrecht, 1989).
14. W. Shockley, *J. Chem. Phys.* **6**:130 (1938).
15. A. Danielian, *Phys. Rev.* **133**:1344 (1964).
16. D. Styer, M. K. Phani, and J. L. Lebowitz, *Phys. Rev. B* **34**:3361 (1986).
17. Y. G. Sinaï, *Theory of Phase Transitions: Rigourous Results* (Pergamon Press, Oxford, 1982).
18. J. Slawny, *J. Stat. Phys.* **20**:711 (1979).
19. J. Slawny, in *Phase Transitions and Critical Phenomena*, Vol. 11, C. Domb and J. L. Lebowitz, eds. (Academic Press, New York, 1987).
20. A. Finel, Thesis, Université Pierre et Marie Curie, Paris, France (1987).
21. J. Bricmont and J. Slawny, *J. Stat. Phys.* **54**:89 (1989).
22. H. Meirovitch, *Phys. Rev. B* **30**:2866 (1984).
23. N. A. Metropolis, A. W. Rosenbluth, M. N. Rosenbluth, A. H. Teller, and E. Teller, *J. Chem. Phys.* **21**:1087 (1953).
24. Y. Saito, K. Furuta, and M. Hoyou, *J. Phys. Soc. Japan* **56**:178 (1987).